

Microcavity Formation in Engineering Polymers Exposed to Hot Water

L. M. ROBESON and S. T. CRISAFULLI, *Union Carbide Corporation,
Research and Development, Bound Brook, New Jersey 08805*

Synopsis

Microcavity formation in engineering polymers exposed to boiling water has recently been noted in the technical literature. This study describes this observation and presents photomicrographs of the microcavity morphology. The microcavities are lens-shaped cracks emitting from a nucleation site with regular concentric ridges observed at regular intervals with characteristics similar to fatigue cracking. Cyclic exposure [intervals of hot (96°C) followed by cold (23°C) water immersion] was found to significantly increase the microcavity formation in specific polymers. Polymers studied under these conditions included polycarbonate, polysulfone, poly(ether sulfone), and polyetherimide. Only polycarbonate and polyetherimide exhibited internal crack formation. The microcavities of polyetherimide were quite different than those of polycarbonate as the cracks were concentrated in regions of highest molded-in stress. When polysulfone was purposely spiked with 0.1 wt % NaCl inclusions, microcavity formation was observed but at a magnitude significantly lower than that of polycarbonate (unmodified). A hypothesis is presented to explain this failure mechanism in polycarbonate. Localized regions (nucleation sites) of higher water solubility can result in higher internal pressure and stress-induced hydrolysis causing microcavity formation. Additional internal pressure (cyclic conditions) can result from water phase separation yielding further crack propagation. Polycarbonate exhibits a larger difference in equilibrium water solubility between 23°C and 96°C than do the other polymers studied, thus yielding a greater potential for internal pressure resulting from phase separation.

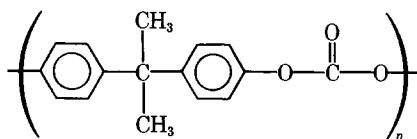
INTRODUCTION

In many end-use applications, engineering polymers encounter various hot, humid environments. Common examples include steam sterilization, boiling water exposure, and dishwashing cycles. Polycarbonate subjected to similar conditions has been studied and reported in various technical papers.¹⁻⁶ These papers clearly demonstrate the loss in mechanical properties of polycarbonate due to the lowering of the molecular weight caused by hydrolysis of the carbonate linkages. More recently, microcavity formation has been reported⁷ under certain water exposure conditions for polycarbonate. Visible disc-shaped microcavities were observed in polycarbonate specimens subjected to boiling water and subsequently stored in water at room temperature. In another recent paper,⁸ microcavities were observed in polycarbonate injection-molded bars after several days exposure to boiling water.

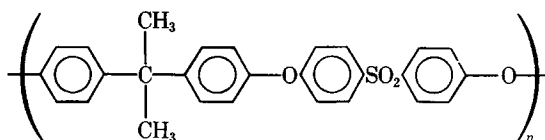
The microcavity formation of crosslinked polymers exposed to boiling water has been reported previously by Fedors for silicone rubber⁹ and epoxy,¹⁰ both containing water-soluble inclusions. The formation of microcavities was considered to be due to the osmotic pressure created by the dissolving inclusion, and an analysis of this process was presented by Fedors.¹¹ He concluded that this

behavior appeared to be a general phenomenon. This behavior was also proposed to be a contributing factor in the water treeing fracture phenomenon observed in power cable insulation.¹²

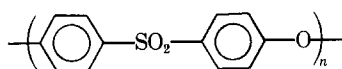
We have also observed the microcavity formation in polycarbonate exposed to various hot, humid conditions and will detail our observations of this behavior in this paper. Additionally, three other engineering polymers were also subjected to equivalent hot water conditioning and will likewise be discussed. The structural formulas for the four polymers included in this study are:



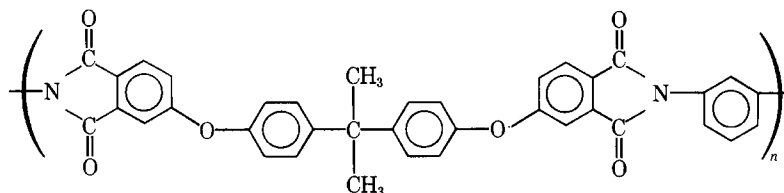
bisphenol A polycarbonate



bisphenol-A-based polysulfone



poly(ether sulfone)



polyetherimide (structure reported in Ref. 13)

Very little is reported in the technical literature on the exposure of bisphenol-A-based polysulfone, poly(ether sulfone), and polyetherimide to hot, humid environments. However, bisphenol-A-based polysulfone has been reported to exhibit a useful creep modulus in steam at or below 130°C somewhat beyond 100,000 h (extrapolated data¹⁴), and end-use applications reported by the manufacturer indicate a myriad of hot, humid environments (e.g., coffee makers, microwave cookware, steam-sterilizable medical equipment). Poly(ether sulfone) and polyetherimide have been reported by their respective trade literature to exhibit utility in hot, humid environments.

A particularly interesting aspect of this study involves the microscopic observation of individual microcavities produced in polycarbonate. These microcavities exhibit a uniform "fatiguelike" failure mechanism which is illustrated by photomicrographs showing circular ridges emitting from the initiation site of microcavitation.

EXPERIMENTAL

Sample Description

The bisphenol A polycarbonate (hereafter referred to as polycarbonate) utilized was Lexan 101 (General Electric Co.). The bisphenol-A-based polysulfone (hereafter referred to as polysulfone) used was UDEL P-1700 (Union Carbide Corp.). The poly(ether sulfone) used was Victrex 200 P (ICI). The polyetherimide used was Ultem 1000 (General Electric Co.). The specimens (unless designated otherwise) for this study were prepared by injection molding under conditions recommended by the material suppliers. The specimens (0.125 in. thick, 0.5 in. wide tensile bars, and flexure bars) were tested for mechanical properties according to the relevant ASTM test procedures.

Samples were placed in a Pyrex beaker containing distilled water and heated on a hot plate to a temperature of $96^{\circ}\text{C} \pm 2^{\circ}\text{C}$. One experimental variable involved cycling the exposure time. This procedure involved approximately 8 h at 96°C followed by cooling to ambient temperature (generally overnight), reheating, and continuing this cycle.

The photomicrographs were obtained utilizing the Reichert optical microscope. The samples were photographed using polarized transmitted illumination.

Experimental Results

The initial experiment involved exposure of polycarbonate, polysulfone, and polyetherimide tensile bar specimens to a cyclic experiment of 65 cycles of 8 h water exposure at 96°C followed by 16–64 h room temperature water immersion. After the cyclic exposure, continuous exposure up to 1700 h total immersion time at 96°C was reached. Samples were periodically taken out and visually observed and stored at 23°C , 50% RH for future reference. Within 50 h exposure time at 96°C (less than seven cycles); microcavities were visually observed in polycarbonate. The size and concentration of these microcavities increased as the exposure time lengthened. After 1700 h, no visual microcavities were observed in the polysulfone specimens. With polyetherimide, cracks parallel to the direction of flow at regions of highest molded-in stress (determined by crosspolarized light patterns) were observed after 200 h exposure. The polycarbonate microcavities appear random throughout the specimen, both in concentration and orientation thus quite different from polyetherimide. Specimens which have been stored at 23°C , 50% RH for over 9 months exhibit no obvious healing of the microcavities for polycarbonate or internal cracks for polyetherimide unlike the results reported by Narkis and Bell.⁷ Perhaps the longer exposure time and/or cyclic nature of our experiment produced irreversible damage. The macroscopic nature of the specimens (before and after 1250 h exposure at 96°C) are shown in Figure 1 for polycarbonate, Figure 2 for polysulfone, and Figure 3 for polyetherimide. Individual microcavities for polycarbonate are illustrated in Figures 4 and 5. The topology of the polycarbonate microcavity is extremely interesting, as illustrated in the photomicrographs. The microcavities have uniform circular ridges emitting from the crack nucleation site with features characteristic of fatigue failure. Microscopic observations of a large number

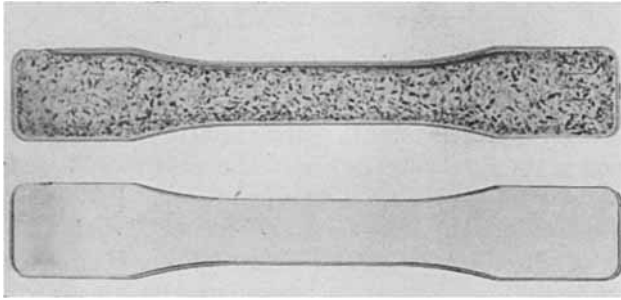


Fig. 1. Polycarbonate tensile specimens before (bottom) and after (top) 1250-h exposure to 96°C water immersion.

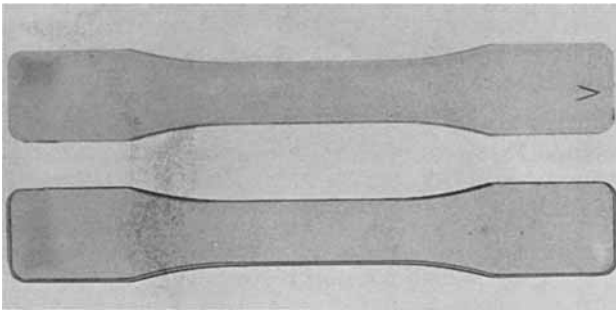


Fig. 2. Polysulfone tensile specimens before (bottom) and after (top) 1250-h exposure to 96°C water immersion (> for identification).

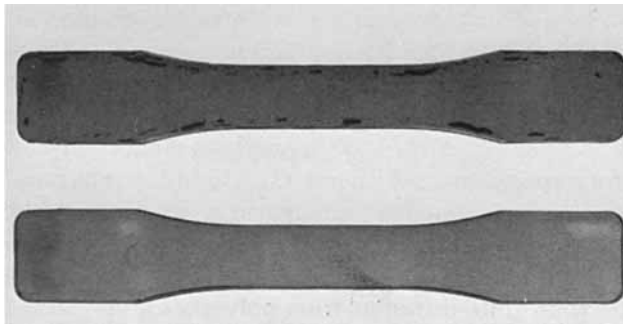


Fig. 3. Polyetherimide tensile specimens before (bottom) and after (top) 1250-h exposure to 96°C water immersion.

of these microcavities revealed the same overall feature with the center of the microcavity (nucleation site) often appearing to be a microscopic impurity. Internal cracks are illustrated in Figure 6 for polyetherimide. The topology of these cracks is quite different from the polycarbonate microcavities.

In the second experiment, injection-molded specimens of polycarbonate, polysulfone, poly(ether sulfone) and polyetherimide were subjected to continuous 96°C water exposure in excess of 3000 h (several changes of distilled water did interrupt the continuous nature of this experiment).

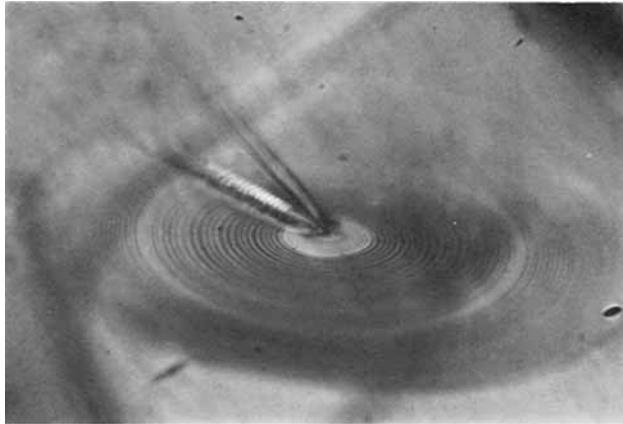


Fig. 4. Photomicrograph (140 \times) of individual microcavity in polycarbonate (cyclic exposure) (1250 h at 96°C water immersion).

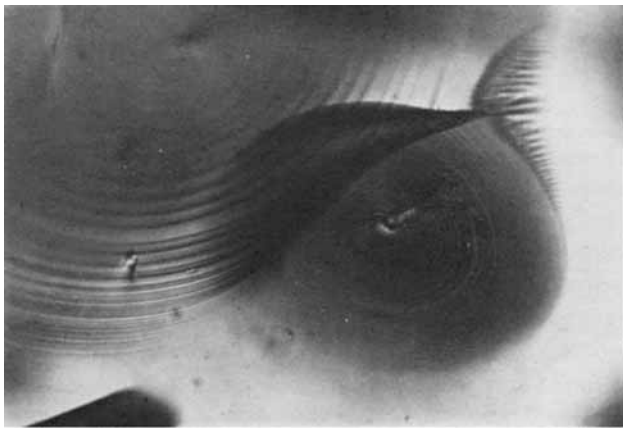


Fig. 5. Photomicrograph (290 \times) of microcavities in polycarbonate (cyclic exposure) (1250 h at 96°C water immersion).

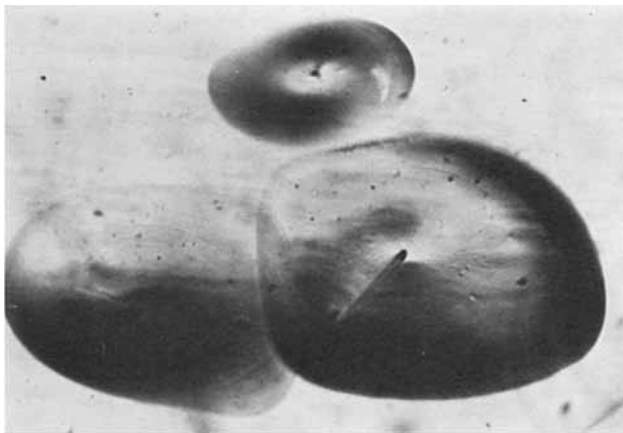


Fig. 6. Photomicrograph (290 \times) of microcavities in polyetherimide (cyclic exposure) (1250 h at 96°C water immersion).

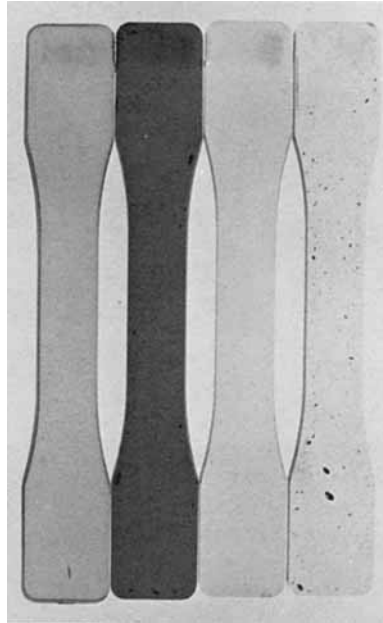


Fig. 7. Tensile specimens of (from left to right) poly(ether sulfone), polyetherimide, polysulfone, and polycarbonate after continuous exposure for 1250 h at 96°C in water [mark at bottom of poly(ether sulfone) specimen is for identification].

The tensile specimens after an exposure interval of 1250 h at 96°C are shown in Figure 7. Microcavities are observed in polycarbonate and internal cracks are present in polyetherimide. The polysulfone and poly(ether sulfone) specimens exhibit no visual change relative to the controls. The one mark on the poly(ether sulfone) sample is a scribe mark made for identification purposes. A photomicrograph of a polycarbonate microcavity is illustrated in Figure 8. As with the cyclic experiment, circular ridges and valleys emit from the point of crack initiation. Note that the severity of the microcavities in polycarbonate and the

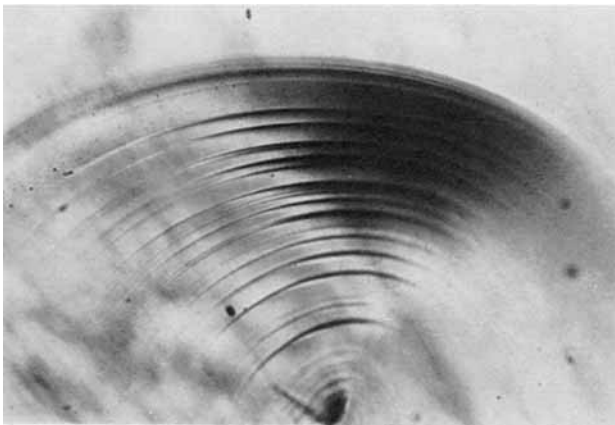


Fig. 8. Photomicrograph (290X) of individual microcavity in polycarbonate (continuous exposure) (1250 h at 96° water immersion).

TABLE I
Mechanical Property (Immersion in 96°C Water)

	Initial	264 h	720 h	1560 h	2020 h	2524 h	3000 h
Polycarbonate							
Tensile strength ^a (MPa)	74	67	69	66	38	13.2	9.0
Notched Izod impact strength ^b (J/m)	929	132		73			
Tensile impact strength ^c (kJ/m ²)	549			15			d
Polysulfone							
Tensile strength ^a (MPa)	72	75	78	81	81	81	82
Notched Izod impact strength ^b (J/m)	70	83		57			
Tensile impact strength ^c (kJ/m ²)	281			229			254
Poly(ether sulfone)							
Tensile strength ^a (MPa)	80	86	83	88	91	93	91
Notched Izod impact strength ^b (J/m)	88	87		63			
Tensile impact strength ^c (kJ/m ²)	316			101			e
Polyetherimide							
Tensile strength ^a (MPa)	112	107	107	109	108	105	94
Notched Izod impact strength ^b (J/m)	64	61		61			
Tensile impact strength ^c (kJ/m ²)	128			58			41

^a Tensile strength determined as per ASTM D-638.

^b Notched Izod impact strength determined as per ASTM D-256.

^c Tensile impact strength determined as per ASTM D-1822.

^d Samples were too brittle to test.

^e No samples available for testing.

internal cracks in polyetherimide are considerably less for the continuous exposure conditioning relative to the cyclic exposure (compare Fig. 1 vs. Fig. 7).

Mechanical property data on these materials at various exposure intervals are listed in Table I. Polycarbonate exhibits the most significant property change with a rapid drop in notched impact strength and a lowering of tensile strength after 1500 h. The initial rapid drop in notched toughness is believed to be due to an annealing process which is similar to that observed for annealing in air at elevated temperatures for short periods of time.^{15,16} The position at which the tensile strength starts to drop is believed due to hydrolysis, yielding a lowered molecular weight combined with microcavity formation, causing flaws in the structure. After 2000 h continuous exposure, the tensile impact strength of polycarbonate has been drastically reduced whereas polysulfone still retains a value characteristic of a tough material. Poly(ether sulfone) and polyetherimide exhibit an intermediate level of tensile impact strength retention. In comparison of the specimens from this continuous experiment with the cyclic experiment, it was quite apparent that the microcavity formation in polycarbonate was significantly less pronounced for the continuous experiment. This was also reflected in tensile strength values as polycarbonate after 555 h in the cyclic experiment had a tensile strength of 53 MPa whereas considerably longer exposure times were required in the continuous experiment to reach that level. In the continuous mode, polyetherimide exhibited internal crack development similar to that reported for the cyclic experiment. Polysulfone and poly(ether sulfone), however, did not exhibit any visual microcavity or internal crack development.

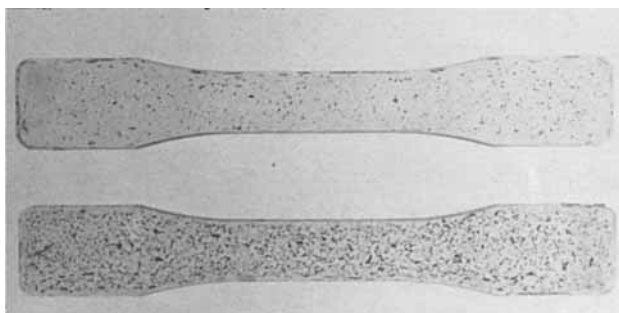


Fig. 9. Comparison of tensile specimens of polycarbonate after (top) continuous exposure (1056 h at 96°C in water) and (bottom) cyclic exposure (256 h at 96°C in water).

The above observation prompted a direct comparison of polycarbonate exposed to continuous and cyclic experiments. Samples were placed in the same Pyrex beaker containing distilled water and heated to 96°C. For cyclic exposure, samples were removed after every 8 h exposure and stored in distilled water for 16 h. After two cycles, microcavity formation was observed in the injection-molded polycarbonate samples. Although the exposure time at 96°C for polycarbonate specimens under continuous conditioning was much greater than that for the cyclic exposure, microcavity formation was significantly more prevalent for samples subjected to cyclic conditions, as illustrated in Figure 9.

As water-soluble inclusions have been noted to cause microcavity formation in epoxy,¹⁰ polycarbonate and polysulfone tensile bars containing 0.1 wt % NaCl were prepared. A concentrated solution of NaCl in water was added to the pellets, followed by thorough drying. The resultant products as well as control specimens were injection-molded followed by cycling in water (8 h at 96°C; 16–64 h at room temperature). Under these conditions, microcavity formation was observed in polysulfone containing 0.1 wt % NaCl but at a much lower concentration and size than either the polycarbonate containing 0.1 wt % NaCl or the control polycarbonate. The polysulfone control specimens exhibited no visual microcavity formation, as noted in the previous experiments. The polycarbonate seeded with NaCl visually appeared to have more severe microcavity formation than the control polycarbonate. This experiment therefore agrees with the

TABLE II
Diffusion and Water Sorption Data

		Diffusion coefficient D (cm ² /s)	Equilibrium water sorption (wt %)
Polycarbonate	23°C	6.5×10^{-8}	0.41
Polycarbonate	96°C	1.0×10^{-6}	0.63
Polysulfone	23°C	3.8×10^{-8}	0.86
Polysulfone	96°C	5.9×10^{-7}	1.00
Poly(ether sulfone)	23°C	1.9×10^{-8}	2.40
Poly(ether sulfone)	96°C	3.6×10^{-7}	2.27
Polyetherimide	23°C	7.8×10^{-9}	1.38
Polyetherimide	96°C	1.6×10^{-7}	1.41

hypothesis of Fedors¹⁰ that this type of failure appears to be a general phenomenon.

The water sorption and diffusion data were determined on compression molded specimens (0.125 in. thick) at 23°C and at 96°C. The equilibrium sorption data (determined by direct weight measurements) are listed in Table II. The diffusion coefficients were determined from q_t/q_∞ data obtained under the following initial and boundary conditions:

$$C = C_0, \quad x = 0, t \geq 0$$

$$C = C_0, \quad x = l, t \geq 0$$

$$C = 0, \quad 0 < x < l, t = 0$$

The value for (t/l^2) when $q_t/q_\infty = 0.5$ can be utilized to calculate the diffusion coefficient as follows:

$$\frac{q_t}{q_\infty} = 1 - \sum_{n=0}^{\infty} \frac{8}{(2n+1)^2\pi^2} e^{-D(2n+1)^2\pi^2t/4l^2}$$

The value for (t/l^2) when $q_t/q_\infty = 0.5$ can be utilized to calculate the diffusion coefficient as follows:

$$D = 0.049/(t/l^2)_{1/2}$$

This assumes a diffusion coefficient which is not concentration-dependent, which is a reasonable assumption for the comparative purposes of this paper. The q_t/q_∞ data at 96°C are illustrated in Figure 10 (23°C) and Figure 11 (96°C) for the four polymers discussed in this paper. The diffusion coefficient data are listed in Table II along with equilibrium sorption data. Poly(ether sulfone) exhibits the highest water sorption followed by polyetherimide whereas polycarbonate exhibits the lowest water sorption. The magnitude of water sorption therefore cannot be used to explain the microcavity formation in polycarbonate

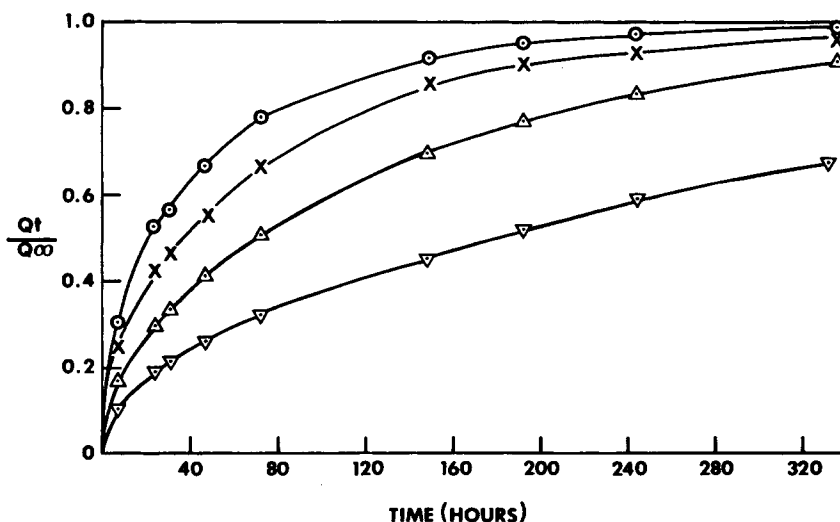


Fig. 10. Water sorption data at 23°C ($1/8$ -in. thick compression molded plaques). (○) Polycarbonate; (×) polysulfone; (△) poly(ether sulfone); (▽) polyetherimide.

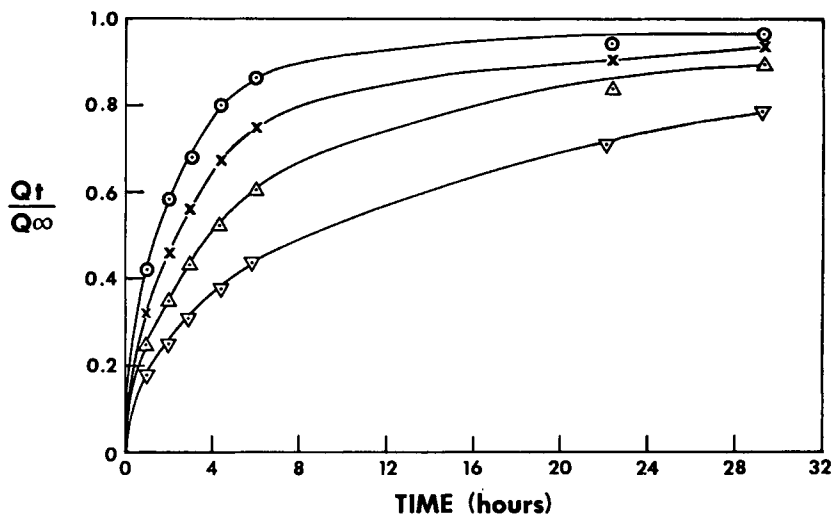


Fig. 11. Water sorption data at 96°C ($\frac{1}{8}$ -in. thick compression molded plaques). (○) Polycarbonate; (×) polysulfone; (△) poly(ether sulfone); (▽) polyetherimide.

as polysulfone and poly(ether sulfone) exhibit higher water sorption values. However, it is of importance to point out that the difference in equilibrium solubility between 96°C and 23°C is greatest for polycarbonate. This will translate into a more significant supersaturated condition for polycarbonate as it is cooled from 96°C to 23°C in a water environment. The potential for internal phase separation would therefore be considered larger for polycarbonate relative to the other polymers. The diffusion coefficient data (at both 23°C and 96°C) follows the trend: polycarbonate > polysulfone > poly(ether sulfone) > polyetherimide.

Discussion of Results

The exposure of polycarbonate to hot (near boiling) water leads to microcavity formation. The morphology of these microcavities is typified by a nucleation site from which regular concentric ridges are observed quite similar to a fatigue fracture pattern. Cyclic exposure to hot water leads to a significantly higher level of microcavity formation than continuous exposure. The nucleus of each microcavity appears to be a region of inhomogeneity (e.g., microscopic particle). The results of Fedors⁹⁻¹² indicate that osmotic pressure can yield microcavity formation in polymers containing water-soluble inclusions. The polycarbonate utilized for these investigations has not been analyzed for specific water-soluble impurities; however, extraction data determined during water diffusion measurements indicate that the water-soluble impurity concentration is probably quite low. Polysulfone under equal exposure conditions does not exhibit microcavity formation unless purposely spiked with a water soluble inclusion.

Cyclic exposure (exhibiting a pronounced severity of microcavity formation over continuous exposure) provides a clue to the origin of microcavity formation. As the polycarbonate specimen is cooled, the equilibrium solubility of water in the specimen decreases before diffusion out of the specimen occurs. The trapped

water can therefore phase-separate at specific nucleation sites. Note that evidence of water clustering in polycarbonate has been experimentally observed.^{18,19} This phase separation can lead to positions of localized pressure. This internal stress potential was hypothesized by Narkis and Bell⁷ as leading to microcavity formation in the polycarbonate samples they tested. Polymeric chains under stressed conditions are more amenable to chemical reaction (e.g., hydrolysis). With polycarbonate, the combination of localized stress combined with potential hydrolysis may lead to crack formation. As the crack forms, the stress is relieved as the internal pressure of the phase-separated water decreases, thus leading to crack growth termination. As the internal pressure of the phase-separated water has decreased with crack formation, more water can diffuse to the crack site, leading to increasing pressure until the crack undergoes further growth. This cyclic behavior thus yields the concentric ridges (and valleys) observed in the microcavities. It is hypothesized that polysulfone and poly(ether sulfone) do not exhibit microcavity formation as the internal pressure created by phase-separated water is not sufficient to promote hydrolytic attack in these polymers.

The equilibrium water solubility for polycarbonate is lower than the other polymers discussed in this paper at both 23°C and 96°C. However, polycarbonate exhibits the largest change in equilibrium water solubility between 96°C and 23°C. This result leads to a more pronounced supersaturation condition for polycarbonate as it is cooled from 96°C to 23°C in water, thus offering a greater magnitude of water phase separation in polycarbonate relative to the other polymers.

Cyclic exposure is much more pronounced than continuous exposure in promoting microcavity formation in polycarbonate as the cyclic condition leads to nonequilibrium conditions yielding water phase separation. Continuous exposure does, however, yield microcavity formation in polycarbonate possibly due to regions of higher water concentration (clustering) and increased hydrolytic attack. As hydrolysis occurs, the byproducts of polycarbonate hydrolysis are CO₂ and two polymer chains with phenol end groups.² This result will lead to further localized H₂O solubility due to the presence of the polar phenol end groups. Regions of increased hydrolytic attack will exhibit increased water solubility and a potential buildup in internal pressure leading to a cascading result, causing microcavity formation.

The observation of the concentric circles emitting from the microcavity nucleus has been noted for metal alloys as well as various plastics.²⁰ It has been shown that the concentric bands represent periods of crack growth and do not particularly represent loading cycles. In fact, a single loading cycle can produce these fatigue striations in various polymers including polycarbonate.²¹ Discontinuous crack growth was noted in a polycarbonate fatigue fracture surface²² with a morphology quite similar to the polycarbonate microcavities noted in this paper.

Polyetherimide also exhibits internal crack formation upon hot water (96°C) exposure. The characteristics of these cracks are quite different than polycarbonate. The cracks are concentrated at regions of highest molded-in stress (~0.0625 in. from the exterior of injection-molded bars). Polycarbonate microcavities are generally random in orientation and are dispersed throughout the specimen.

Microcavity formation does not occur in polysulfone or poly(ether sulfone) under the conditions of the experiments noted here. Polysulfone spiked with 0.1 wt % NaCl inclusions, however, does exhibit microcavity formation, although the size and concentration is considerably less than that observed in polycarbonate (either as is or also spiked with 0.1 wt % NaCl). These results are in agreement with observations of Fedors,⁹⁻¹² where microcavity formation in polymers containing water-soluble inclusions was noted.

The mechanical property results indicate that cyclic exposure is more detrimental to tensile strength retention in polycarbonate than continuous exposure in a hot, humid environment. The lowering of properties of polycarbonate exposed to hot water immersion is due to three separate causes: (1) initial lowering of toughness due to an annealing effect similar to that observed by annealing in air at temperatures approaching the T_g ; (2) hydrolysis, leading to molecular weight reduction, resulting in material embrittlement; (3) microcavity formation, producing structural flaws, offering sites for crack initiation before ductile yielding can occur.

References

1. R. J. Gardner and J. R. Martin, *J. Appl. Polym. Sci.*, **24**, 1269 (1979).
2. C. A. Pryde and M. Y. Hellman, *J. Appl. Polym. Sci.*, **25**, 2573 (1980).
3. J. W. Shea, C. J. Aloisio, and R. R. Cammons, SPE 35th ANTEC, Montreal, Canada, April 25-28, 1977, p. 326.
4. H. E. Bair, D. R. Falcone, M. Y. Hellman, G. E. Johnson, and P. G. Kelleher, *Polym. Prepr. Am. Chem. Soc., Div. Polym. Chem.*, **20**(2), 614 (1979).
5. C. A. Pryde, P. G. Kelleher, M. Y. Hellman, and R. P. Wentz, *Polym. Eng. Sci.*, **22**, 370 (1982).
6. P. G. Kelleher, R. P. Wentz, M. Y. Hellman, and E. H. Gilbert, SPE 40th ANTEC, San Francisco, May 10-12, 1982, p. 111.
7. M. Narkis and J. P. Bell, *J. Appl. Polym. Sci.*, **27**, 2809 (1982).
8. E. A. Joseph, D. R. Paul, and J. W. Barlow, *Am. Chem. Soc., Div. Org. Coat. Appl. Polym. Sci.*, **47**, 272 (1982); *J. Appl. Polym. Sci.*, **27**, 4807 (1982).
9. R. F. Fedors, *J. Polym. Sci., Polym. Lett. Ed.*, **12**, 81 (1974).
10. R. F. Fedors, *Polymer*, **21**, 713 (1980).
11. R. F. Fedors, *Polymer*, **21**, 207 (1980).
12. R. F. Fedors, *Polymer*, **21**, 863 (1980).
13. S. A. White, S. R. Weissman, and R. P. Kambour, *J. Appl. Polym. Sci.*, **27**, 2675 (1982).
14. R. K. Dearing, SPE 34th ANTEC, Atlantic City, N.J., April 1976.
15. L. J. Broutman and S. M. Krishnakumar, *Polym. Eng. Sci.*, **16**, 74 (1976).
16. D. C. Prevorsek, Y. Kesten, and B. DeBona, *Polym. Prepr., Am. Chem. Soc., Div. Polym. Chem.*, **20**(1), 187 (1979).
17. J. Crank, *The Mathematics of Diffusion*, Oxford University Press, London, 1956.
18. G. E. Johnson, H. E. Bair, and S. Matsuoka, in *Water in Polymers*, S. P. Rowland, Ed., ACS Symposium Series 127, Washington, D. C., 1980, p. 451.
19. H. E. Bair, G. E. Johnson, and R. Merriweather, *J. Appl. Phys.*, **49**, 4976 (1978).
20. R. W. Hertzberg and J. A. Manson, in *Fatigue of Engineering Plastics*, Academic, New York, 1980.
21. M. D. Skiko, R. W. Hertzberg, J. A. Manson, and S. Kim, *J. Mater. Sci.*, **12**, 531 (1977).
22. M. T. Takemori and D. S. Matsumoto, *J. Polym. Sci., Polym. Phys. Ed.*, **20**, 2027 (1982).

Received February 2, 1983

Accepted May 9, 1983